Hellings-Downs curve deformed by ultralight vector dark matter

Omiya, Hidetoshi
Nomura, Kimihiro
Soda, Jiro

(Citation)
Physical Review D,108(10):104006

(Issue Date)
2023-11-15

(Resource Type)
journal article

(Version)
Version of Record

(URL)
https://hdl.handle.net/20.500.14094/0100486280

Hellings-Downs curve deformed by ultralight vector dark matter

Hidetoshi Omiya[*] and Kimihiro Nomura[†]
Department of Physics, Kobe University, Kobe 657-8501, Japan

Jiro Soda[‡]
Department of Physics, Kobe University, Kobe 657-8501, Japan
and International Center for Quantum-field Measurement Systems for Studies of the Universe and Particles (QUP), KEK, Tsukuba 305-0801, Japan

(Received 31 July 2023; accepted 12 October 2023; published 3 November 2023)

Pulsar timing arrays (PTAs) provide a way to detect gravitational waves (GWs) at nanohertz frequencies. To ensure the detection of GWs, observational data must exhibit the Hellings-Downs angular correlation. It is also known that PTAs can probe ultralight dark matter. This paper considers possible contamination of the Hellings-Downs angular correlation by the ultralight dark matter. We find that ultralight vector dark matter can give rise to the deformation of the Hellings-Downs correlation curve. Thus, the Hellings-Downs correlation curve could contain information on ultralight dark matter with a spin.

DOI: 10.1103/PhysRevD.108.104006

I. INTRODUCTION

The first direct detection of gravitational waves (GWs) by LIGO [1] has initiated GW astronomy. To further develop GW astronomy, observing GWs in a different frequency range is crucial. Intriguingly, pulsar timing arrays (PTAs) provide a way to detect gravitational waves (GWs) at nanohertz frequencies [2]. A requirement for claiming the detection of GWs [3] is to verify Hellings-Downs angular correlation [4]. Recently, evidence of stochastic GWs has been reported [5–9]. In particular, the angular correlation seems to follow the Hellings-Downs pattern.

Curiously, PTAs can also explore the ultralight dark matter. Ultralight dark matter is a model of dark matter realized by the coherent oscillation of an ultralight bosonic field, with its frequency given by the mass of the field. This coherent oscillation will then lead to fluctuations of the gravitational potential, which cause the timing residual of the pulses from the pulsar [10]. Since PTAs are sensitive to the nanohertz frequency band, the mass around 10^{-24} eV $\lesssim \mu \lesssim 10^{-22}$ eV can be explored. Indeed, the energy density of axion dark matter has been constrained by pulsar timing observations [11–13].

Although the axion dark matter is more popular for its simplicity, there is a possibility of ultralight vector dark matter [14,15]. The interesting feature of vector dark matter is introducing a particular direction determined by the local direction of the vector field. Remarkably, it turns out that signals of ultralight vector dark matter in PTAs are strongly anisotropic due to this feature [16,17].

Observationally, it is true that GWs and dark matter coexist. Hence, it is important to clarify the effect of ultralight dark matter on the Hellings-Downs correlation. However, the axion dark matter cannot produce a feature in angular correlation due to its scalar nature. On the other hand, the vector dark matter has the potential to induce a nontrivial angular correlation pattern since a coherently oscillating vector field defines a specific direction. Thus, the Hellings-Downs curve might be contaminated by the vector dark matter.

For this purpose, we examine the angular correlation of PTAs in the coexistence of GWs and vector dark matter. By calculating the cross-correlation signal from the pulsars, we find that the vector dark matter induces the mixture of the monopole and the quadrupole angular correlation pattern. Therefore, the Hellings-Downs correlation is deformed by the vector dark matter. It is expected that the same happens for any dark matter with spin. Hence, the Hellings-Downs correlation tells us not only the existence of GWs but also that of ultralight dark matter.

The organization of the paper is as follows. In Sec. II, we evaluate pulsar timing residual induced by ultralight vector dark matter. In Sec. III, we calculate the angular correlation of pulsar timing signals and show that the Hellings-Downs curve will be deformed by the vector dark matter. In Sec. IV, we summarize this paper. We fix our units to $c = \hbar = 1$ in the following.

[*]h.omiya@people.sci.kobe-u.ac.jp
[†]knomura@stu.sci.kobe-u.ac.jp
[‡]jiro@phys.sci.kobe-u.ac.jp

II. PULSAR TIMING RESIDUAL INDUCED BY VECTOR DARK MATTER

In this paper, we focus on the ultralight vector dark matter denoted by A_μ. The coherence length of the vector field is estimated to be

$$\lambda_{\rm dB} = \frac{2\pi}{\mu v_{\rm DM}} \sim 0.4\ {\rm kpc}\left(\frac{10^{-22}\ {\rm eV}}{\mu}\right)\left(\frac{10^{-3}}{v_{\rm DM}}\right), \quad (1)$$

where μ is the mass of the ultralight field and $v_{\rm DM}$ is the typical velocity of the dark matter particle in the unit of the speed of light. Another important number is the occupation number of the dark matter particle, which is roughly calculated to be

$$N_{\rm DM} \sim \frac{\rho_{\rm DM}}{\mu}\lambda_{\rm dB}^3 \sim 10^{93}\left(\frac{\rho_{\rm DM}}{0.4\ {\rm GeV\,cm^{-3}}}\right)\left(\frac{10^{-22}\ {\rm eV}}{\mu}\right)^4\left(\frac{10^{-3}}{v_{\rm DM}}\right)^3. \quad (2)$$

This huge occupation number allows us to treat the ultralight field as a classical field.

The action of the vector dark matter A_μ is given by

$$S = \int d^4x\sqrt{-g}\left(-\frac{1}{4}F_{\mu\nu}F^{\mu\nu} - \frac{1}{2}\mu^2 A_\mu A^\mu\right), \quad (3)$$

with

$$F_{\mu\nu} = \nabla_\mu A_\nu - \nabla_\nu A_\mu. \quad (4)$$

Taking variation of the action, we obtain the equation of motion for A_μ as

$$\nabla_\mu F^{\mu\nu} - \mu^2 A^\nu = 0. \quad (5)$$

Since $F_{\mu\nu}$ is antisymmetric, the divergence of Eq. (5) leads to

$$\nabla_\mu A^\mu = 0, \quad (6)$$

which immediately gives

$$A^0 \sim \frac{1}{\mu\lambda_{\rm dB}}A^i. \quad (7)$$

Here we utilized the fact that the typical scale of the spatial variation of the field is $\sim\lambda_{\rm dB}$, and the vector field is coherently oscillating with frequency μ. Since $\mu\lambda_{\rm dB} = 2\pi/v_{\rm DM} \gg 1$, we can neglect the zeroth component of the vector field.

To summarize, we can approximate the vector field configuration to be

$$A_0 = 0, \quad \boldsymbol{A}(t,\boldsymbol{x}) = \boldsymbol{\Omega}_A(\boldsymbol{x})A(\boldsymbol{x})\cos(\mu t + \alpha(\boldsymbol{x})), \quad (8)$$

where $A(\boldsymbol{x})$ is the amplitude of the field, which is related to the dark matter density as

$$\rho_{\rm DM} \sim \frac{\mu^2}{2}A^2(\boldsymbol{x}), \quad (9)$$

$\boldsymbol{\Omega}_A(\boldsymbol{x})$ is a unit vector pointing to the direction of the vector field, and $\alpha(\boldsymbol{x})$ describes the spatial dependence of the field. Note that the spatial gradient of the field is on the scale of $2\pi/\lambda_{\rm dB} = \mu v_{\rm DM}$, which is much smaller than μ. In the following, we assume

$$\alpha(\boldsymbol{x}) = \boldsymbol{k}\cdot\boldsymbol{x} \quad (10)$$

with $|\boldsymbol{k}| \ll \mu$. Here, we treated the field as completely monochromatic since the expected width of the frequency should be much smaller than the frequency resolution of pulsar timing observations [5–9]. We also emphasize that we are neglecting the stochastic nature of the ultralight dark matter.

The coherent oscillation of the vector dark matter produces the fluctuations of the metric. Solving Einstein equations in the weak field limit, we obtain [18]

$$ds^2 = -(1-2\Psi(t,\boldsymbol{x}))dt^2 + [(1+2\Psi(t,\boldsymbol{x}))\delta_{ij} + \gamma_{ij}(t,\boldsymbol{x})]dx^i dx^j, \quad (11)$$

with

$$\Psi(t,\boldsymbol{x}) = \Psi_{\rm osc}(\boldsymbol{x})\cos(2\mu t + 2\boldsymbol{k}\cdot\boldsymbol{x}), \quad (12)$$

$$\gamma_{ij}(t,\boldsymbol{x}) = h_{\rm osc}(\boldsymbol{x})(\delta_{ij} - 3\Omega_{A,i}(\boldsymbol{x})\Omega_{A,j}(\boldsymbol{x}))\cos(2\mu t + 2\boldsymbol{k}\cdot\boldsymbol{x}), \quad (13)$$

$$\Psi_{\rm osc}(\boldsymbol{x}) = -\frac{\pi G}{6}A^2(\boldsymbol{x}), \quad (14)$$

$$h_{\rm osc}(\boldsymbol{x}) = \frac{4\pi G}{3}A^2(\boldsymbol{x}) = -8\Psi_{\rm osc}(\boldsymbol{x}). \quad (15)$$

Here we only considered the time-dependent parts, which affect the observed periodicity of pulses from pulsars. The details of deriving Eq. (11) can be found in [16].

The metric fluctuations induce a redshift of the observed pulses from pulsars. The observed redshift of pulses at time t from the pulsar a is defined by

$$z_a(t) = \frac{\omega_{0,a} - \omega_{{\rm obs},a}(t)}{\omega_{0,a}}, \quad (16)$$

where $\omega_{0,a}$ is the intrinsic angular frequency of pulses emitted from the pulsar a, and $\omega_{{\rm obs},a}(t)$ is the observed angular frequency of pulses which are affected by metric

perturbations. Because of the metric perturbations (11), the redshift is given by [19]

$$z_a(t) = \int_{t-L_a}^{t} dt' \left[\frac{\partial}{\partial t'}\Psi(t', \boldsymbol{x})\right]_{\boldsymbol{x}=\boldsymbol{x}_a(t')} + \frac{1}{2} u_a^i u_a^j \int_{t-L_a}^{t} dt' \left[\frac{\partial}{\partial t'}\gamma_{ij}(t', \boldsymbol{x})\right]_{\boldsymbol{x}=\boldsymbol{x}_a(t')}, \quad (17)$$

where $\boldsymbol{x}_a(t') = (t - t')\boldsymbol{u}_a + \boldsymbol{x}_{\rm E}$ with $\boldsymbol{x}_{\rm E}$ being the position of the Earth, and L_a is the distance to the pulsar a from the Earth. Here, $\boldsymbol{u}_a$ is a unit vector pointing to the pulsar a.

By substituting Eq. (11) into Eq. (17), we obtain [16]

$$\begin{aligned} z_a(t) \approx{}& \Psi_{\rm osc}(\boldsymbol{x}_{\rm E})\cos(2\mu t + 2\boldsymbol{k}\cdot\boldsymbol{x}_{\rm E}) \\ &- \Psi_{\rm osc}(\boldsymbol{x}_a)\cos(2\mu t - 2\mu L_a + 2\boldsymbol{k}\cdot\boldsymbol{x}_a) \\ &+ \frac{1}{2} h_{\rm osc}(\boldsymbol{x}_{\rm E})(1 - 3(\boldsymbol{u}_a\cdot\boldsymbol{\Omega}_{A,{\rm E}})^2)\cos(2\mu t + 2\boldsymbol{k}\cdot\boldsymbol{x}_{\rm E}) \\ &- \frac{1}{2} h_{\rm osc}(\boldsymbol{x}_a)(1 - 3(\boldsymbol{u}_a\cdot\boldsymbol{\Omega}_{A,a})^2) \\ &\times \cos(2\mu t - 2\mu L_a + 2\boldsymbol{k}\cdot\boldsymbol{x}_a) \\ ={}& F^{\rm DM}_{a,{\rm E}}\Psi_{\rm osc}(\boldsymbol{x}_{\rm E})\cos(2\mu t + 2\boldsymbol{k}\cdot\boldsymbol{x}_{\rm E}) \\ &- F^{\rm DM}_{a,{\rm P}}\Psi_{\rm osc}(\boldsymbol{x}_a)\cos(2\mu t - 2\mu L_a + 2\boldsymbol{k}\cdot\boldsymbol{x}_a), \end{aligned} \quad (18)$$

where $\boldsymbol{x}_{\rm E}$ is the position of the Earth, $\boldsymbol{x}_a$ is the position of the pulsar a, and $\boldsymbol{\Omega}_{A,{\rm E}} = \boldsymbol{\Omega}_A(\boldsymbol{x}_{\rm E})$ and $\boldsymbol{\Omega}_{A,a} = \boldsymbol{\Omega}_A(\boldsymbol{x}_a)$ are the directions of the vector field at the Earth and the pulsar a, respectively. Here, we introduced the beam pattern functions in the presence of the vector dark matter as

$$\begin{aligned} F^{\rm DM}_{a,{\rm E}} &= -3(1 - 4(\boldsymbol{u}_a\cdot\boldsymbol{\Omega}_{A,{\rm E}})^2), \\ F^{\rm DM}_{a,{\rm P}} &= -3(1 - 4(\boldsymbol{u}_a\cdot\boldsymbol{\Omega}_{A,a})^2). \end{aligned} \quad (19)$$

The beam pattern functions are functions of the angle between the direction to the pulsar $\boldsymbol{u}_a$ and the direction of the vector field $\boldsymbol{\Omega}_{A,{\rm E}/a}$. We show the angular dependence of $F^{\rm DM}_{a,{\rm E/P}}$ in Fig. 1. We observe that the beam pattern functions of the dark matter show a quadrupole pattern.

The timing residual $\Delta T_a(t)$ of the pulsar a can be obtained from the redshift as

$$\Delta T_a(t) = \int_0^t dt' z_a(t'). \quad (20)$$

After performing the integral in Eq. (20), we obtain

$$\begin{aligned} \Delta T_a(t) = \frac{1}{2\mu}&(F^{\rm DM}_{a,{\rm E}}\Psi_{\rm osc}(\boldsymbol{x}_{\rm E})\sin(2\mu t + 2\boldsymbol{k}\cdot\boldsymbol{x}_{\rm E}) \\ &- F^{\rm DM}_{a,{\rm P}}\Psi_{\rm osc}(\boldsymbol{x}_a)\sin(2\mu t - 2\mu L_a + 2\boldsymbol{k}\cdot\boldsymbol{x}_a)). \end{aligned} \quad (21)$$

Note that the origin of time can be taken arbitrarily. We see that the ultralight vector field will induce a timing residual oscillating with a frequency 2μ.

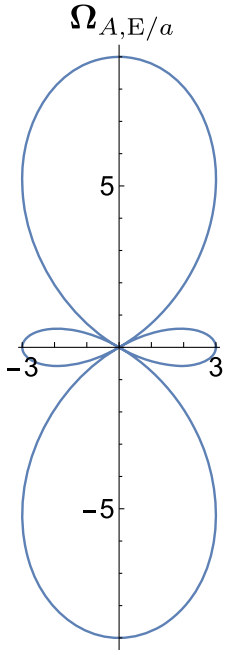

FIG. 1. The angular dependence of the beam pattern functions $F^{\rm DM}_{a,{\rm E/P}}$ is depicted. The direction of the vector field $\boldsymbol{\Omega}_{A,{\rm E}/a}$ is taken to be along the vertical axis, and the angle $\boldsymbol{u}_a\cdot\boldsymbol{\Omega}_{A,{\rm E}/a}$ is measured from the vertical axis.

III. DEFORMATION OF HELLINGS-DOWNS ANGULAR CORRELATION

The essential ingredient to detect the GW background is taking the cross-correlation between the noise-independent data [2,4,20,21]. By taking the cross-correlation, the signal is enhanced relative to the noise. The cross-correlation between the timing residuals of the pulsar a and b can be calculated through

$$C_{ab}(\tau) \equiv \langle \Delta T_a(t)\Delta T_b(t+\tau)\rangle - \langle \Delta T_a(t)\rangle\langle \Delta T_b(t+\tau)\rangle. \quad (22)$$

Here, $\langle\cdots\rangle$ means a time average or an ensemble average. We start with briefly reviewing the angular correlation produced by the gravitational wave background, which is known as the Hellings-Downs curve in Sec. III A. Then, in Sec. III B, we give the derivation of the angular correlation from the vector dark matter. Finally, in Sec. III C, we show how the Hellings-Downs are deformed in the case when the gravitational wave background and the vector dark matter coexist.

A. Angular correlation by the gravitational wave background

For the stationary, isotropic, unpolarized, and Gaussian GW background, the cross-correlation can be computed analytically [4]. The result is

$$C_{ab}^{\mathrm{SGWB}}(\tau) = \sum_i \Gamma_{\mathrm{HD}}(\xi)\Phi_{\mathrm{GW}}(f_i)\cos 2\pi f_i \tau, \quad (23)$$

with

$$\Phi_{\mathrm{GW}}(f_i) = \frac{1}{12\pi^2 f_i^3}\frac{1}{T_{\mathrm{obs}}} h_c^2(f_i). \quad (24)$$

Note that we discretized the frequency integral into the sum of the frequency bins determined by the observation time T_{obs}, as in [5]. Here, Γ_{HD} is the Hellings-Downs curve given by

$$\Gamma_{\mathrm{HD}}(\xi) = \frac{1}{2} + \frac{3}{2}\left(\frac{1-\cos\xi}{2}\right)\log\left(\frac{1-\cos\xi}{2}\right) - \frac{1}{4}\left(\frac{1-\cos\xi}{2}\right) \quad (25)$$

with ξ being the angular separation between pulsar a and b, and h_c is the characteristic strain amplitude of the stochastic GW background defined by

$$\langle h_P(f,\boldsymbol{\Omega}) h^*_{P'}(f',\boldsymbol{\Omega}')\rangle = \frac{h_c^2(f)}{16\pi f}\delta(f-f')\delta_{PP'}\delta(\boldsymbol{\Omega}-\boldsymbol{\Omega}'). \quad (26)$$

The characteristic strain is related to the energy density spectrum normalized by the critical density of the universe $\Omega_{\mathrm{GW}}(f)$ as [22]

$$\Omega_{\mathrm{GW}}(f) = \frac{2\pi^2}{3H_0^2} f^2 h_c^2(f), \quad (27)$$

where H_0 denotes the Hubble constant. It is conventional to parametrize the characteristic strain as

$$h_c(f) = A_{\mathrm{GW}}\left(\frac{f}{f_{\mathrm{ref}}}\right)^{\alpha} \quad (28)$$

with a reference frequency f_{ref}. Then, Eq. (24) is rewritten as

$$\Phi_{\mathrm{GW}}(f_i) = \frac{A_{\mathrm{GW}}^2}{12\pi^2}\frac{1}{T_{\mathrm{obs}}}\left(\frac{f_i}{f_{\mathrm{ref}}}\right)^{-\gamma} f_{\mathrm{ref}}^{-3}, \quad (29)$$

where $\gamma = -2\alpha + 3$.

B. Angular correlation by the ultralight vector dark matter

Now let us proceed to calculate the cross-correlation signal of the vector dark matter. When taking the time average, one should note that $\mu^{-1} \lesssim 10$ yr for the dark matter with the mass $\mu \gtrsim 10^{-24}$ eV. This means that after the time average over the observational period ($T_{\mathrm{obs}} \sim 10$ yr), oscillating terms such as $\cos(2\mu t)$ vanish. We also take an average over the observed pulsars. This operation effectively makes our analysis parallel to the case of the stochastic background, despite our focus on the deterministic fluctuation of the vector dark matter (see Refs. [23–25] for the case of black hole binaries which produces the deterministic signal).

With this in mind, we substitute Eq. (21) to Eq. (22) and take the time average to obtain

$$\begin{aligned}
&\langle \Delta T_a(t)\Delta T_b(t+\tau)\rangle \\
&= \frac{1}{2(2\mu)^2}[\langle \Psi_{\mathrm{osc}}(\boldsymbol{x}_a)\Psi_{\mathrm{osc}}(\boldsymbol{x}_b)\rangle\langle F_{a,\mathrm{P}}^{\mathrm{DM}} F_{b,\mathrm{P}}^{\mathrm{DM}}\rangle \\
&\quad\times\cos(2\mu\tau + 2\mu(L_a - L_b) - 2\boldsymbol{k}\cdot(\boldsymbol{x}_a - \boldsymbol{x}_b)) \\
&\quad - \langle \Psi_{\mathrm{osc}}(\boldsymbol{x}_{\mathrm{E}})\Psi_{\mathrm{osc}}(\boldsymbol{x}_b)\rangle\langle F_{a,\mathrm{E}}^{\mathrm{DM}} F_{b,\mathrm{P}}^{\mathrm{DM}}\rangle \\
&\quad\times\cos(2\mu\tau - 2\mu L_b - 2\boldsymbol{k}\cdot(\boldsymbol{x}_{\mathrm{E}} - \boldsymbol{x}_b)) \\
&\quad - \langle \Psi_{\mathrm{osc}}(\boldsymbol{x}_{\mathrm{E}})\Psi_{\mathrm{osc}}(\boldsymbol{x}_a)\rangle\langle F_{a,\mathrm{P}}^{\mathrm{DM}} F_{b,\mathrm{E}}^{\mathrm{DM}}\rangle \\
&\quad\times\cos(2\mu\tau + 2\mu L_a - 2\boldsymbol{k}\cdot(\boldsymbol{x}_a - \boldsymbol{x}_{\mathrm{E}})) \\
&\quad + \langle \Psi_{\mathrm{osc}}^2(\boldsymbol{x}_{\mathrm{E}})\rangle\langle F_{a,\mathrm{E}}^{\mathrm{DM}} F_{b,\mathrm{E}}^{\mathrm{DM}}\rangle\cos 2\mu\tau]. \quad (30)
\end{aligned}$$

The first three terms are the pulsar-related terms. Since we are averaging over the pulsars, we need to take the average with respect to the distance to the individual pulsar. Notably, the observed pulsars lie in the range 0.1 kpc $\lesssim L \lesssim$ 10 kpc, which corresponds to $10 \lesssim \mu L \lesssim 10^3$ for $\mu = 10^{-24}$ eV. Thus, after averaging over distance to the pulsar, the pulsar-related terms are relatively suppressed to the Earth term. As pointed out in the case of the gravitational waves from the individual source, the suppressed pulsar terms act as the noise [24]. The resulting expression after taking the average over the distance to the pulsar is

$$\begin{aligned}
&\langle \Delta T_a(t)\Delta T_b(t+\tau)\rangle \\
&\quad\approx \frac{1}{2(2\mu)^2}\langle \Psi_{\mathrm{osc}}^2(\boldsymbol{x}_{\mathrm{E}})\rangle\langle F_{a,\mathrm{E}}^{\mathrm{DM}} F_{b,\mathrm{E}}^{\mathrm{DM}}\rangle\cos 2\mu\tau. \quad (31)
\end{aligned}$$

The pulsars we observe are distributed all over the sky; thus, their relative angle to the direction of the vector field is completely random. This means that the average of the cross-correlation signals among many pulsars effectively takes an average over the direction of the vector field $\boldsymbol{\Omega}_A$. This is parallel to the gravitational wave background originating from the binary black holes (see, for example, Fig. 2 of [23]). The averaging over the directions of the pulsars is the crucial step that makes the result analogous to the stochastic background. One can simulate in a similar manner as [26] that if we can observe enough number of pulsars [for example, $\mathcal{O}(10^2)$, which is easily achieved in the future [27,28]], this angular averaging procedure gives

a good approximation. In the Appendix, we provide the simulation of the angular correlation.

To calculate the angular dependence of the cross-correlation signal, we choose the coordinate system such that $\boldsymbol{u}_a = (0, 0, 1)$ and $\boldsymbol{u}_b = (\sin\xi, 0, \cos\xi)$. In this coordinate system, we can easily perform the integral over $\boldsymbol{\Omega}_A$ to obtain

$$\begin{aligned}\langle F^{\rm DM}_{a,{\rm E}} F^{\rm DM}_{b,{\rm E}}\rangle &= 9\int \frac{d\boldsymbol{\Omega}_A}{4\pi}(1-4(\boldsymbol{u}_a\cdot\boldsymbol{\Omega}_{A,{\rm E}})^2)\\ &\quad\times(1-4(\boldsymbol{u}_b\cdot\boldsymbol{\Omega}_{A,{\rm E}})^2)\\ &= \frac{3}{5}(7+16\cos 2\xi) \equiv \frac{138}{5}\Gamma_{\rm DM}(\xi). \end{aligned} \tag{32}$$

Here,

$$\Gamma_{\rm DM}(\xi) = \frac{5}{138}P_0(\cos\xi) + \frac{64}{138}P_2(\cos\xi) \tag{33}$$

shows the angular correlation between the pulsars, and we normalized it such that $\Gamma_{\rm DM}(0) = 1/2$. Equation (33) shows that the vector field will introduce a mixture of the monopole and the quadrupole angular correlation pattern.

The two main differences between the vector dark matter signal and the gravitational wave signal are the presence of the monopole pattern and the absence of the multipole modes beyond the quadrupole. The presence of the monopole pattern is obvious since the massive vector field includes the scalar mode. The absence of the higher multipole modes is due to the standing wave nature of the vector dark matter. Note that the higher multipole modes in the gravitational wave signal are induced by the propagation of the gravitational wave [25].

To summarize, the cross-correlation signal produced by the ultralight vector field is given by

$$C^{\rm DM}_{ab}(\tau) = \Gamma_{\rm DM}(\xi)\Phi_{\rm DM}\cos 2\mu\tau, \tag{34}$$

where

$$\Phi_{\rm DM} = \frac{69}{5(2\mu)^2}\langle\Psi^2_{\rm osc}(\boldsymbol{x}_{\rm E})\rangle. \tag{35}$$

In Fig. 2, the Hellings-Downs pattern due to stochastic GWs, $\Gamma_{\rm HD}(\xi)$, is drawn by a red solid curve, and the angular correlation pattern produced by the vector dark matter, $\Gamma_{\rm DM}(\xi)$, is drawn by a blue dashed curve. We observe the angular correlation produced by the vector dark matter is dominated by the quadrupole, which is evident from the expression (33) (see also Fig. 1).

C. Total angular correlation

Now let us consider when the gravitational wave background and the ultralight vector coexist. In this case, the total timing residual is given as the sum of two signals

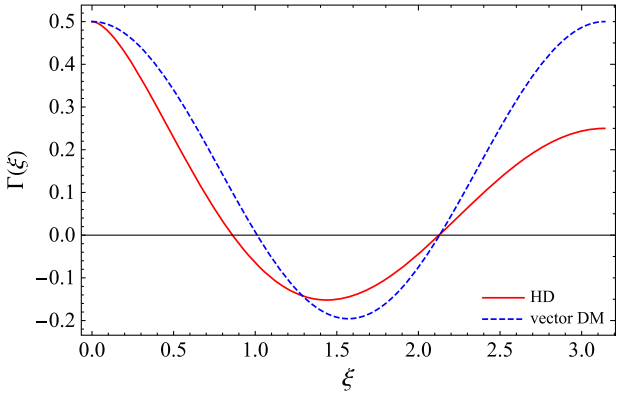

FIG. 2. The red solid and blue dashed curves correspond to the angular correlation of the timing residuals induced by the gravitational wave background (Hellings-Downs curve) and the ultralight vector dark matter, respectively.

$$\Delta T_{{\rm tot},a} = \Delta T_{{\rm GW},a} + \Delta T_{{\rm DM},a} + N_a. \tag{36}$$

Here, we neglect the noise term, which vanishes when we take the cross-correlation. The cross-correlation of the total signal is given by

$$\begin{aligned}\langle\Delta T_{{\rm tot},a}(t)\Delta T_{{\rm tot},b}(t+\tau)\rangle &= \langle\Delta T_{{\rm GW},a}(t)\Delta T_{{\rm GW},b}(t+\tau)\rangle\\ &\quad+\langle\Delta T_{{\rm DM},a}(t)\Delta T_{{\rm DM},b}(t+\tau)\rangle.\end{aligned} \tag{37}$$

Here, the cross term is dropped since the gravitational wave background and the vector dark matter should be independent. Thus, the total correlation signal is given by the sum of the signal from GWs and the ultralight vector dark matter, which is

$$\begin{aligned}C_{ab}(\tau) &= \sum_i \Gamma_{\rm HD}(\xi)\Phi_{\rm GW}(f_i)\cos 2\pi f_i\tau\\ &\quad+\Gamma_{\rm DM}(\xi)\Phi_{\rm DM}\cos 2\mu\tau.\end{aligned} \tag{38}$$

Now, we define the effective overlap reduction function $\Gamma_{\rm eff}$ at the frequency band which includes $2\pi f = 2\mu$ as

$$\begin{aligned}\Gamma_{\rm eff}(\xi) &= \frac{\Phi_{\rm GW}(\mu/\pi)}{\Phi_{\rm GW}(\mu/\pi)+\Phi_{\rm DM}}\\ &\quad\times\left(\Gamma_{\rm HD}(\xi)+\frac{\Phi_{\rm DM}}{\Phi_{\rm GW}(\mu/\pi)}\Gamma_{\rm DM}(\xi)\right).\end{aligned} \tag{39}$$

The normalization is chosen so that $\Gamma_{\rm eff}(0) = 1/2$. This quantity shows how the Hellings-Downs curve is deformed by the presence of the ultralight vector dark matter.

For $A_{\rm GW}$ introduced in Eq. (28), the NANOGrav obeservation [5] reported $A_{\rm GW} = 2.4\times10^{-15}$ at $\gamma = 13/3$ with $T_{\rm obs}\sim 15$ yr and $f_{\rm ref} = 1\ {\rm yr}^{-1}$. Using this value, through Eq. (29), $\Phi_{\rm GW}$ at $f = \mu/\pi$ is estimated to be

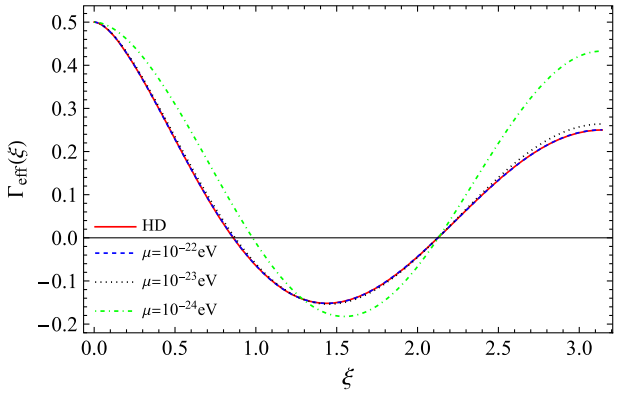

FIG. 3. The blue dashed, the black dotted, and the green dot-dashed curves correspond to $\Gamma_{\rm eff}(\xi)$ for $\mu = 10^{-22}, 10^{-23}$, and 10^{-24} eV, respectively. Here, we take $\rho_{\rm DM} = 0.4$ GeV cm^{-3} and $T_{\rm obs} = 15$ yr. For reference, we show the Hellings-Downs curve in the red solid curve.

$$\Phi_{\rm GW}(\mu/\pi) \sim 5 \times 10^{-34}\ {\rm yr}^2 \left(\frac{\mu}{10^{-22}\ {\rm eV}}\right)^{-13/3} \left(\frac{15\ {\rm yr}}{T_{\rm obs}}\right). \quad (40)$$

On the other hand, assuming the dark matter is composed solely of the ultralight dark matter and neglecting the stochastic effect [29], we can estimate $\Phi_{\rm DM}$ as

$$\Phi_{\rm DM} \sim 7 \times 10^{-37}\ {\rm yr}^2 \left(\frac{\rho_{\rm DM}}{0.4\,{\rm GeV\,cm^{-3}}}\right)^2 \left(\frac{10^{-22}\ {\rm eV}}{\mu}\right)^6. \quad (41)$$

In Fig. 3, we show $\Gamma_{\rm eff}$ for several values of the ultralight dark matter mass μ. Our result shows that the presence of the ultralight vector field will deform the angular correlation pattern from the Helling-Downs curve if the vector field mass is as light as $\mu \sim 10^{-23}$ eV. However, for the heavier vector field mass, the contribution from the dark matter is negligible, and thus no characteristic feature from the dark matter can be easily observed.

IV. CONCLUSION

The Hellings-Downs correlation plays a central role in confirming the existence of stochastic gravitational waves (GWs). Hence, it is important to clarify possible contamination from other effects. Given that pulsar timing arrays (PTAs) are sensitive both to GWs and ultralight dark matter at nanohertz frequencies, it is necessary to examine the effect of ultralight dark matter on PTA angular correlations. For this reason, we studied the Hellings-Downs angular correlation in the presence of GWs and ultralight vector dark matter.

Our main finding is that a deformation of the Hellings-Downs correlation curve can be induced by ultralight vector dark matter at the frequency $f = \mu/\pi$ if the dark matter mass is in the range 10^{-24} eV $\lesssim \mu \lesssim 10^{-23}$ eV. This deformation can be a clear signature of the ultralight vector dark matter. For the higher dark matter mass, the contamination due to the dark matter is small enough; thus, the Hellings-Downs curve is maintained.

We should mention that our result is based on neglecting the stochastic nature of the ultralight dark matter and assumption on the uniform distribution of the observed pulsar all over the sky. The stochastic nature has been extensively discussed for the ultralight scalar dark matter [29]. For the scalar dark matter, the stochastic effect would effectively reduce the amplitude from the naive estimation of the local dark matter density. For the vector dark matter, in addition to the amplitude, the direction of the vector field also fluctuates [30]. Since we are effectively averaging over the direction of the vector field, the fluctuation of the vector direction should have no effect.

The uniform distribution of the pulsars all over the sky is a crucial assumption of this work. However, observed pulsars do not distribute uniformly across the sky. The average over the nonuniform distribution might result in deformation of the angular correlation since the integrand in Eq. (32) will be changed. We leave a detailed investigation on the impacts of the stochastic nature of the ultralight dark matter and the nonuniform nature of the observed pulsars on the angular correlation for future work.

This paper focused on the angular correlation pattern produced by the vector dark matter. Let us now discuss possible applications of our findings. The immediate application is to constrain the vector dark matter by the angular correlation of PTAs. In the previous literature, the angular correlation induced by ultralight dark matter has been ignored. Since the angular correlation would provide more information, the constraint should be strengthened. Also, it is possible to consider the prospect of separately observing the GW background and the dark matter in a similar way to the decomposition of polarization components in the GW background [26,31,32].

Although we have concentrated on the spin-1 matter, extending the analysis to higher spin matters is straightforward. For example, there have been some attempts to consider the spin-2 matter as dark matter [33–37]. Moreover, the pulsar timing residual has been calculated with higher spin fields [38–40]. The higher spin fields should produce different angular correlation patterns, which can be used to constrain them.

Another simple extension of our work is to consider anisotropic components of the signal. Since the vector dark matter naturally introduces the specific direction, there should be a strong anisotropy in pulsar timing signals. We leave these issues for future work.

ACKNOWLEDGMENTS

We are grateful to the referee for his/her suggestions to improve the manuscript. H. O. was supported by JSPS KAKENHI Grant No. JP22J14159. K. N. was supported

by JSPS KAKENHI Grant No. JP21J20600. J. S. was in part supported by JSPS KAKENHI Grants No. JP17H02894, No. JP17K18778, No. JP20H01902, and No. JP22H01220.

APPENDIX: SIMULATION OF THE AVERAGING PROCEDURE

To demonstrate that our averaging procedure is justified, we simulated the situation by generating 50, 100, and 200 random pulsars over the sky. The distance to each pulsar is taken log uniformly in the range $0.1\ \mathrm{kpc} \leq L \leq 10\ \mathrm{kpc}$. We also fix our ultralight dark matter mass to be $\mu = 10^{-24}$ eV. This corresponds to $10 < \mu L < 10^3$. The angular correlation is calculated by taking the mean of

$$\begin{aligned} C_{ab}(0) \propto\ & F^{\mathrm{DM}}_{a,\mathrm{P}} F^{\mathrm{DM}}_{b,\mathrm{P}} \cos\left(2\mu(L_a - L_b)\right) \\ & - F^{\mathrm{DM}}_{a,\mathrm{E}} F^{\mathrm{DM}}_{b,\mathrm{P}} \cos(2\mu L_b) \\ & - F^{\mathrm{DM}}_{a,\mathrm{P}} F^{\mathrm{DM}}_{b,\mathrm{E}} \cos(2\mu L_a) \\ & + F^{\mathrm{DM}}_{a,\mathrm{E}} F^{\mathrm{DM}}_{b,\mathrm{E}}. \end{aligned} \tag{A1}$$

Here, we neglected terms involving $\boldsymbol{k}$, since $|\boldsymbol{k}|$ is suppressed by $v \sim 10^{-3}$. We normalize the angular correlation such that the mean value of the autocorrelation becomes unity.

The result is shown in Fig. 4. From Fig. 4, it is obvious by eye that the correlation pattern follows Eq. (33). Also, we observe that pulsar-related terms effectively act as noise terms.

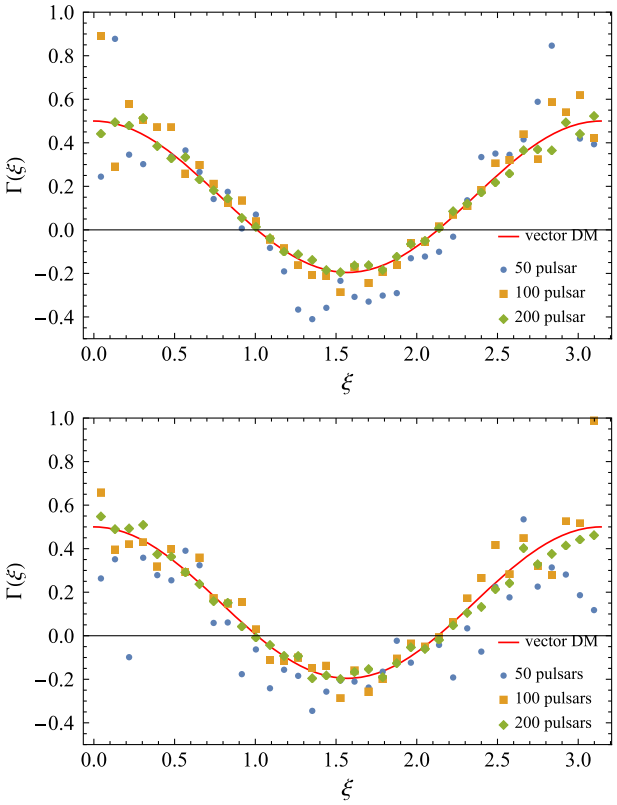

FIG. 4. The top and bottom panels show the simulated angular correlation curve produced by the vector dark matter with and without the pulsar terms, respectively. The blue circle, orange square, and green diamond show three different realizations. The red solid curve shows the correlation given by Eq. (33). We binned the data with width 5°.

[1] B. P. Abbott *et al.* (LIGO Scientific and Virgo Collaborations), Phys. Rev. Lett. **116**, 061102 (2016).
[2] S. L. Detweiler, Astrophys. J. **234**, 1100 (1979).
[3] B. Allen, S. Dhurandhar, Y. Gupta, M. McLaughlin, P. Natarajan, R. M. Shannon, E. Thrane, and A. Vecchio, arXiv:2304.04767.
[4] R. w. Hellings and G. s. Downs, Astrophys. J. Lett. **265**, L39 (1983).
[5] G. Agazie *et al.* (NANOGrav Collaboration), Astrophys. J. Lett. **951**, L8 (2023).
[6] A. Afzal *et al.* (NANOGrav Collaboration), Astrophys. J. Lett. **951**, L11 (2023).
[7] J. Antoniadis *et al.*, Astron. Astrophys. **678**, A50 (2023).
[8] H. Xu *et al.*, Res. Astron. Astrophys. **23**, 075024 (2023).
[9] D. J. Reardon *et al.*, Astrophys. J. Lett. **951**, L6 (2023).
[10] A. Khmelnitsky and V. Rubakov, J. Cosmol. Astropart. Phys. 02 (2014) 019.
[11] N. K. Porayko and K. A. Postnov, Phys. Rev. D **90**, 062008 (2014).
[12] N. K. Porayko *et al.* (PPTA Collaboration), Phys. Rev. D **98**, 102002 (2018).
[13] R. Kato and J. Soda, J. Cosmol. Astropart. Phys. 09 (2020) 036.
[14] A. E. Nelson and J. Scholtz, Phys. Rev. D **84**, 103501 (2011).
[15] K. Nakayama, J. Cosmol. Astropart. Phys. 10 (2019) 019.
[16] K. Nomura, A. Ito, and J. Soda, Eur. Phys. J. C **80**, 419 (2020).
[17] Y.-M. Wu, Z.-C. Chen, Q.-G. Huang, X. Zhu, N. D. R. Bhat, Y. Feng, G. Hobbs, R. N. Manchester, C. J. Russell, and R. M. Shannon (PPTA Collaboration), Phys. Rev. D **106**, L081101 (2022).
[18] It is not obvious that we can bring the metric perturbation to the form (11). However, under the assumption of neglecting the spatial gradient, we can show that it is true. See Ref. [16] for the derivation.
[19] M. Maggiore, *Gravitational Waves: Volume 2: Astrophysics and Cosmology* (Oxford University Press, New York, 2018).
[20] P. F. Michelson, Mon. Not. R. Astron. Soc. **227**, 933 (1987).
[21] E. E. Flanagan, Phys. Rev. D **48**, 2389 (1993).

[22] B. Allen and J. D. Romano, Phys. Rev. D **59**, 102001 (1999).
[23] N. J. Cornish and A. Sesana, Classical Quantum Gravity **30**, 224005 (2013).
[24] B. Allen, Phys. Rev. D **107**, 043018 (2023).
[25] J. D. Romano and B. Allen, arXiv:2308.05847.
[26] N. J. Cornish, L. O'Beirne, S. R. Taylor, and N. Yunes, Phys. Rev. Lett. **120**, 181101 (2018).
[27] L. Shao, I. Stairs, J. Antoniadis, A. Deller, P. Freire, J. Hessels, G. Janssen, M. Kramer, J. Kunz, C. Laemmerzahl, V. Perlick, A. Possenti, S. Ransom, B. Stappers, and W. van Straten, Proc. Sci., AASKA14 (**2015**) 042 [arXiv:1501.00058].
[28] M. Bailes *et al.*, Proc. Sci., MeerKAT2016 (**2018**) 011 [arXiv:1803.07424].
[29] G. P. Centers *et al.*, Nat. Commun. **12**, 7321 (2021).
[30] X. Xue *et al.* (PPTA Collaboration), Phys. Rev. Res. **4**, L012022 (2022).
[31] R. Kato and J. Soda, Phys. Rev. D **93**, 062003 (2016).
[32] E. Belgacem and M. Kamionkowski, Phys. Rev. D **102**, 023004 (2020).
[33] K. Aoki and S. Mukohyama, Phys. Rev. D **94**, 024001 (2016).
[34] K. Aoki and K.-i. Maeda, Phys. Rev. D **97**, 044002 (2018).
[35] E. Babichev, L. Marzola, M. Raidal, A. Schmidt-May, F. Urban, H. Veermäe, and M. von Strauss, J. Cosmol. Astropart. Phys. 09 (2016) 016.
[36] L. Marzola, M. Raidal, and F. R. Urban, Phys. Rev. D **97**, 024010 (2018).
[37] Y. Manita, K. Aoki, T. Fujita, and S. Mukohyama, Phys. Rev. D **107**, 104007 (2023).
[38] S. Sun, X.-Y. Yang, and Y.-L. Zhang, Phys. Rev. D **106**, 066006 (2022).
[39] C. Unal, F. R. Urban, and E. D. Kovetz, arXiv:2209.02741.
[40] Y.-M. Wu, Z.-C. Chen, and Q.-G. Huang, J. Cosmol. Astropart. Phys. 09 (2023) 021.